ACS APPLIED MATERIALS & INTERFACES

LETTER

www.acsami.org

Discriminating between Bilayer and Bulk Heterojunction Polymer: Fullerene Solar Cells Using the External Quantum Efficiency

Veronique S. Gevaerts, L. Jan Anton Koster, Martijn M. Wienk, and René A. J. Janssen*

Molecular Materials and Nanosystems, Eindhoven University of Technology, PO Box 513, 5600 MB Eindhoven, The Netherlands

Supporting Information

ABSTRACT: The morphology of the active layer in polymer:fullerene solar cells is a key parameter for the performance. We compare bilayer poly(3-hexylthiophene)/[6,6]-phenyl-C_{61}-butyric acid methyl ester (P3HT/PCBM) solar cell devices produced from orthogonal solvents before and after thermal annealing with P3HT:PCBM bulk heterojunction solar cells produced from a single solvent. By comparing the spectral shape and magnitude of the experimental and theoretically modeled EQEs we show that P3HT/PCBM bilayers made via orthogonal solution processing do not lead to bilayers with a sharp interface but that partial intermixing has occurred. Thermal annealing of these diffusive P3HT/PCBM bilayers leads to increased mixing but does not result in the same mixed bulk heterojunction morphology that is obtained when P3HT and PCBM are cast simultaneously from single solution. For thicker layers, the annealed bilayers significantly outperform the bulk heterojunction devices with the same nominal composition and same total thickness.

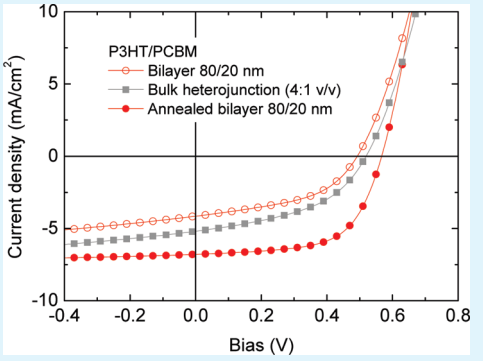

KEYWORDS: solar cell, polythiophene, fullerene, morphology

INTRODUCTION

Efficient organic photovoltaic cells can be made by mixing a semiconducting π−conjugated polymer with fullerene derivative into a bulk heterojunction photoactive layer.[1,2] Such a bulk heterojunction consists of a nanometer scale interpenetrating network of the two materials, formed spontaneously during layer deposition, sometimes assisted by thermal or solvent annealing. Because of the nanometer size exciton diffusion lengths in organic semiconductors, a large interface area between the two components, and hence intimate mixing, is beneficial for dissociating excitons formed under illumination and generating charges. At the same time, the components must form percolating pathways to transport the charges to the electrodes. Charge transport benefits from larger domains. The effects of mixing vs phase separation on performance have been studied in some detail for bulk heterojunction solar cells based on poly(3-hexylthiophene) (P3HT) and [6,6]-phenyl-C_{61}-butyric acid methyl ester (PCBM).[2,3]

Interestingly, Ayzner et al.[4] recently reported that solution processed thermally annealed P3HT/PCBM bilayer solar cells can be almost as efficient as bulk heterojunction cells. In their work an orthogonal solvent combination (*o*-dichlorobenzene and dichloromethane) was used to process a PCBM layer on top of a P3HT layer. Although evidence was presented that this procedure results in real bilayers with a sharp inerface,[4] several recent more detailed investigations, using transmission electron microscopy, X-ray photon electron spectroscopy, time-of-flight secondary-ion mass spectrometry, and X-ray scattering, provide evidence of interdiffusion of PCBM into P3HT producing an intermixed heterojunction directly during deposition.[5−11]

The partial mixing of P3HT and PCBM during deposition of PCBM is caused by swelling of the P3HT in the solvent used to deposit the PCBM. Thermal annealing drives the interdiffusion of P3HT and PCBM to completion.[10,11] During thermal annealing, PCBM becomes miscible and mobile in disordered and amorphous P3HT regions, without disrupting the ordered domains with lamellar stacking of P3HT chains.[7,11]

Here we show that the spectrally resolved external quantum efficiency (EQE) of the solar cell devices can be used as an indicator of bilayer interfacial mixing. We reveal that the EQE of P3HT/PCBM bilayer devices cast from orthogonal solvents is not compatible with a discrete P3HT/PCBM interface and that some intermixing occurs at the interface when depositing the PCBM layer.[5−11] We further demonstrate that annealing of these diffusive P3HT/PCBM bilayers leads to increased mixing but does not result in the same mixed bulk heterojunction morphology that is obtained when P3HT and PCBM are cast simultaneously from single solution. These results are consistent with a recent morphological study of Russell et al. showing that after annealing PCBM is homogenously distributed in the amorphous P3HT regions that separate the crystalline P3HT domains in the film.[11]

EXPERIMENTAL SECTION

P3HT (Plexcore OS 2100, > 98% regioregular) was spun slowly from *o*-dichlorobenzene (ODCB) and dried for at least 20 min.

Received: June 12, 2011
Accepted: July 20, 2011
Published: July 20, 2011

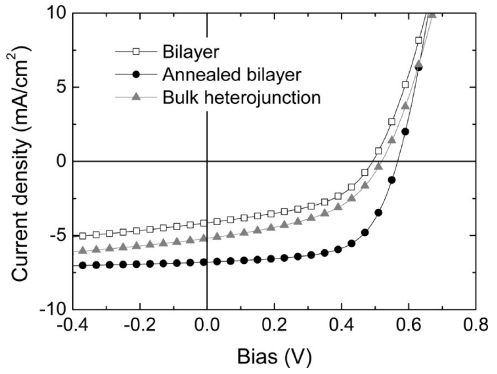

Figure 1. Current density−voltage characteristics of as-cast bilayer, annealed bilayer, and bulk heterojunction cells using 20 nm of PCBM and 80 nm of P3HT.

On top, PCBM (Solenne) was spun from dichloromethane.[4] Three different P3HT layer thicknesses (40, 80, and 120 nm) were used, keeping the thickness of the PCBM layer (20 nm) constant. The thickness of the PCBM layer was limited by the solubility of PCBM in dichloromethane that is used as an orthogonal solvent for the underlying P3HT layers. These bilayers were studied as cast and after annealing at 150 °C in a nitrogen atmosphere for 20 min. Bulk heterojunctions were made using volume ratios (2:1, 4:1, and 6:1) and layer thickness (60, 100, and 140 nm) that allow direct comparison with the bilayers because they nominally have the same thickness and composition. These blends were spun cast from ODCB which evaporates slowly such that a phase-segregated morphology with semicrystalline P3HT and PCBM domains was obtained without annealing. All layers were deposited on glass covered with patterned indium tin oxide (ITO) and poly(3,4-ethylenedioxythiophene): poly(styrenesulfonate) (PEDOT:PSS). Devices were completed by evaporating LiF (1 nm) and Al (100 nm) as back contact in vacuum.

Solar cell characteristics were measured under ~100 mW/cm^2 white light from a tungsten halogen lamp filtered by a Schott GG385 UV filter and a Hoya LB120 daylight filter, using a Keithley 2400 source meter. The external quantum efficiency was measured using monochromatic light from a 50 W tungsten halogen lamp (Philips focusline) in combination with monochromator (Oriel, Cornerstone 130). The response was recorded as the voltage over a 50 Ω resistance, using a lock-in amplifier (Stanford research Systems SR830). A calibrated Si cell was used as reference to obtain external quantum efficiencies. The device was measured in a nitrogen filled box. The thicknesses of the layers in the solar cells were measured on a Veeco Dektak 150 profilometer.

Transmission electron microscopy (TEM) was performed on a Tecnai G^2 Sphera TEM (FEI) operated at 200 kV. Bright field TEM images were acquired under slight defocusing conditions.

RESULTS AND DICUSSION

Figure 1 compares the current density−voltage (J−V) curves of P3HT(80 nm)/PCBM(20 nm) bilayer devices made using dichloromethane as an orthogonal solvent before and after annealing with the performance of an equally thick (100 nm) P3HT:PCBM bulk heterojunction made in a volume ratio of 4:1 (weight ratio of 8:3) that corresponds to the relative thickness of the P3HT and PCBM layers in the as-cast bilayer. The annealed bilayer device outperforms both other devices. The relevant solar cell parameters collected in Table I show that the same conclusion holds for devices with thinner (40 nm) and thicker (120 nm) P3HT layers, although the differences are small for the thin films.

Table I. Short-Circuit Current (J_{sc}), Open-Circuit Voltage (V_{oc}), Fill Factor (FF), and Maximum Power Point (MPP) for As-Cast Bilayer (BL), Annealed Bilayer (A-BL), and Bulk Heterojunction (BHJ) Solar Cells with Different Layer Thicknesses (d) and Volume Ratios of P3HT and PCBM

type	d (nm)	J_{sc} (mA/cm^2)	V_{oc} (V)	FF	MPP (mW/cm^2)
BL	40/20	4.00	0.47	0.49	0.93
A-BL	40/20	4.57	0.49	0.59	1.33
BHJ	60 (2:1)	4.12	0.53	0.62	1.34
BL	80/20	4.15	0.49	0.47	0.96
A-BL	80/20	6.80	0.57	0.62	2.38
BHJ	100 (4:1)	5.20	0.52	0.46	1.23
BL	120/20	2.16	0.48	0.42	0.43
A-BL	120/20	5.34	0.56	0.49	1.46
BHJ	140 (6:1)	2.00	0.47	0.39	0.37

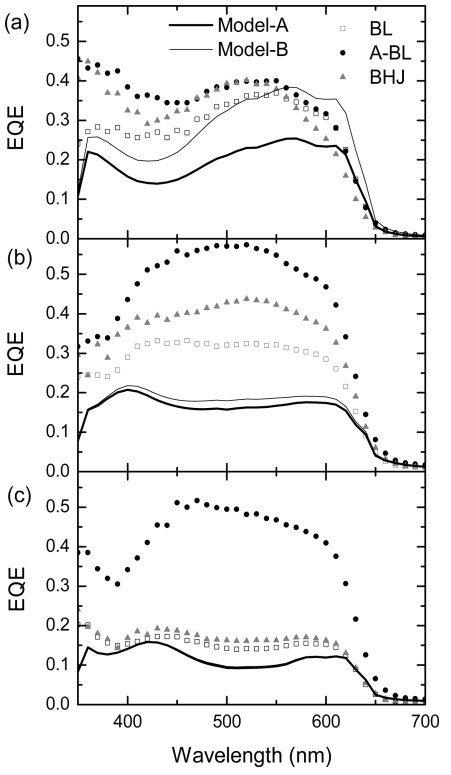

Figure 2. Measured (symbols) and calculated (lines) EQEs for solar cells having 20 nm PCBM and (a) 40, (b) 80, and (c) 120 nm P3HT in bilayer (BL), annealed bilayer (A-BL), and bulk heterojunction (BHJ) configurations. The calculations include (model-A) or exclude (model-B) quenching of P3HT excitons at the PEDOT:PSS electrode.

EQE measurements for the as-cast bilayer, annealed bilayer, and bulk heterojunction layers reveal similar differences (Figure 2). The EQE of the 40/20 as-cast bilayer increases slightly after annealing and the contribution at short wavelength (likely due to PCBM) becomes more important (Figure 2a). After annealing, the EQE resembles that of the bulk heterojunction. For the thicker active layers with volume ratios of 4:1 and 6:1, the changes are

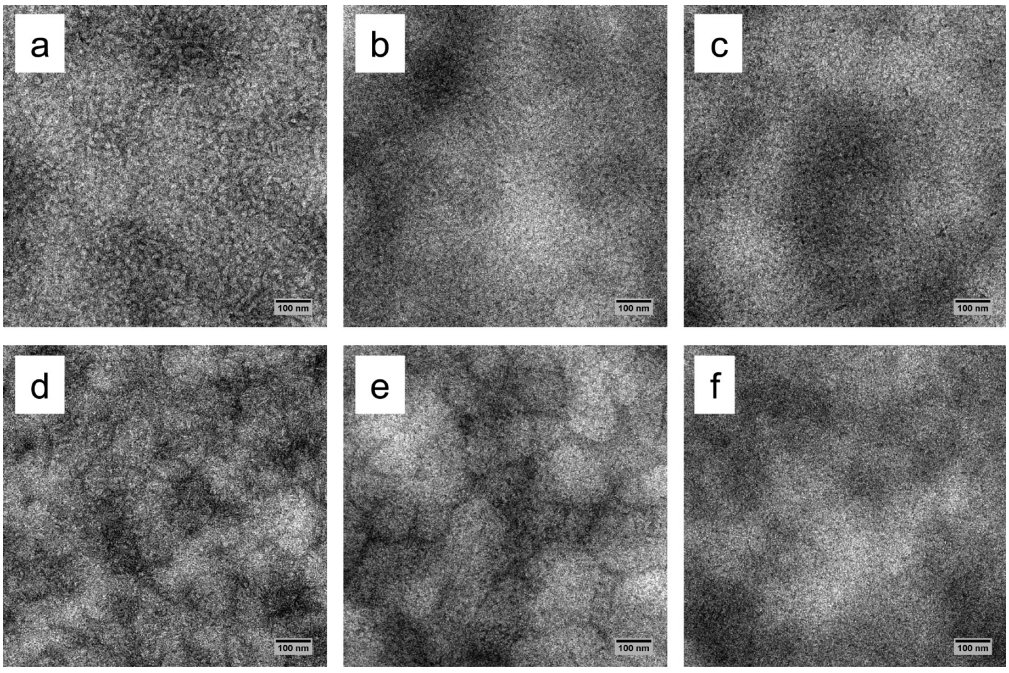

Figure 3. Bright-field TEM images of annealed P3HT/PCBM bilayers (a) 40/20 nm, (b) 80/20 nm, (c) 120/20 nm, and of solution cast P3HT:PCBM bulk heterojunctions (d) 60 nm (2:1 v/v), (e) 80 nm (4:1 v/v), and 140 nm (6:1 v/v).

more dramatic. Annealed bilayers and bulk heterojunctions show strikingly different performance. In both cases, the annealed bilayer reaches a much higher EQE and shows different wavelength dependence. Because the layers have the same composition (P3HT/PCBM ratio) and thickness this demonstrates that thermal annealing of as-cast bilayers produces composite layers that differ from the bulk heterojunction obtained from casting the same mixture from solution.

Bright field TEM images of the annealed bilayers and the solution cast bulk heterojunctions confirm that the morphologies are not the same (Figure 3). For the annealed bilayers (Figure 3a−c) the phase separation produced appears to be finer than for the bulk heterojunctions (Figure 3d−f). The differences are more evident for the thinner films, because in the thicker films the volume concentration of PCBM is small (14%).

To investigate the origin of these EQE differences in more detail, optical modeling was performed on assuming perfect bilayers with a sharp interface. The transfer matrix method was used to calculate exciton generation profiles from the wavelength dependent refractive index (n) and extinction coefficient (k) of P3HT and PCBM (see the Supporting Information). The choice of n and k values for P3HT is important, because they may vary with degree of aggregation, molecular weight, regioregularity, and solvent used. We used a linear combination of functions[12] that accurately reproduced the transmission of both thick and thin P3HT layers cast from ODCB (see the Supporting Information). We further find that for all three as-cast bilayer devices the experimental reflection spectrum accurately matches with the results from the optical modeling when a discrete interface is assumed. This shows that the optical absorption is not very sensitive to the intermixing at the interface and that we can use the optical modeling to determine the number of absorbed photons (see the Supporting Information). Figure 4 shows the calculated exciton generation rate in a P3HT/PCBM bilayer for three selected wavelengths.

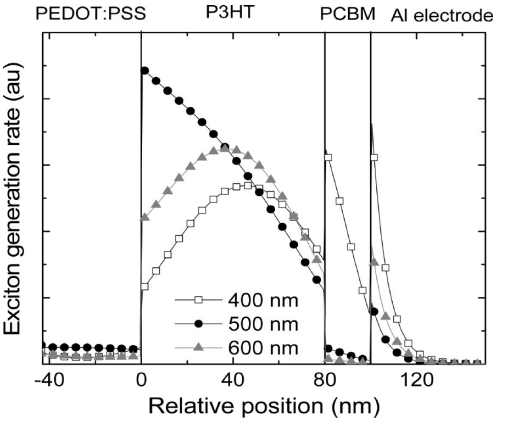

Figure 4. Exciton generation profiles for different wavelengths in a bilayer solar cell with 80 nm P3HT and 20 nm PCBM.

Combining the exciton generation rate profiles with one-dimensional exciton diffusion we calculated the wavelength dependent EQE for perfect bilayers with a sharp interface. The diffusion of excitons in each layer is described by

$$\frac{dn(x)}{dt} = g(x) - \frac{n(x)}{\tau} + D\frac{d^2n(x)}{dx^2} \quad (1)$$

where $g(x)$ is the exciton generation rate, D the exciton diffusion constant, τ is the exciton lifetime, and $n(x)$ the exciton density. The exciton lifetime and diffusion constant in PCBM were taken from the literature:[13] $\tau = 1.25$ ns and $D = 2.0 \times 10^{-8}$ m^2/s, giving a diffusion length of 5 nm. For P3HT different exciton diffusion lengths were considered; the largest value found in literature was $L = 21$ nm, with $\tau = 0.60$ ns and $D = 1.0 \times 10^{-6}$ m^2/s.[14] We assume that excitons are quenched at the P3HT/PCBM interface and at the LiF/Al electrode, such that $n(t) = 0$ at these positions. At the PEDOT:PSS electrode either full (model A)[15] or no

(model B)[16] quenching of excitons was considered. Equation 1 is solved numerically for steady state ($dn(x)/dt = 0$) and from the steady state exciton density profile the number of excitons quenched at the interfaces is determined. The excitons quenched at the P3HT/PCBM interface are assumed to generate charges that contribute to the photocurrent in the solar cell at short circuit without further losses. Because of the short diffusion length in PCBM, excitons generated in P3HT give the main contribution to the current and, hence, the EQE.

The calculations show that even for a relatively large value of L = 21 nm for P3HT, the calculated EQEs of perfect bilayers remain well below the experimental values (Figure 2) of the as-cast samples, irrespective of assuming full (A) and no (B) quenching at the PEDOT:PSS interface. Higher values for L also do not reproduce the experimental data (not shown). We conclude that the use of orthogonal solvents does not produce perfect bilayers and that some intermixing at the P3HT/PCBM interface occurs before annealing, likely caused by swelling of P3HT in the dichloromethane used to cast PCBM.[10] Because the performance of the as-cast 40/20 nm bilayer changes only slightly upon annealing, the diffusion of PCBM into P3HT during deposition is possibly up to 40 nm. The EQE calculations reproduce the minimum at 500 nm for the 80/20 nm and 120/20 nm bilayers (Figure 2b,c). This is a direct consequence of the reduced exciton generation rate near the P3HT/PCBM interface for photons of 500 nm (Figure 4) because only a few photons reach the interface with PCBM as they are attenuated by the absorbing P3HT. This filtering does not occur to the same extent at 400 and 600 nm, where P3HT absorbs less strongly.

Figure 2c shows that the EQE of the annealed P3HT-(120 nm)/PCBM(20 nm) bilayer cell is almost three times higher than the corresponding as-cast bilayer and bulk heterojunction cells and does not show a minimum in the EQE at ~500 nm. For the as-cast bilayer the minimum is directly explained by the optical modeling. Also for the bulk heterojunction, the minimum in EQE is due to an internal filter effect. In the (6:1 v/v) bulk heterojunction, the concentration of PCBM is low, which causes poor percolation pathways for electron transport to the LiF/Al electrode. Electrons generated close to the PEDOT:PSS electrode are therefore likely to recombine before being collected. In contrast, the annealed bilayer shows no obvious filter effects. The large increase in EQE and the change in spectral shape leave no doubt that further intermixing occurs at the P3HT/PCBM interface by annealing and we conjecture that the annealed morphology is neither a real bilayer nor a intimately mixed bulk heterojunction, but rather a morphology in which PCBM is dispersed throughout the P3HT layer in a continuous manner to explain the absence of a filter effect in the EQE and the excellent percolation pathways for electrons. This result is consistent with Figure 3 and with recent morphological studies that imply that PCBM rapidly diffuses into the amorphous P3HT regions that separate the crystalline P3HT domians.[11]

CONCLUSION

EQE measurements in combination with optical modeling can be used as an indicator of bilayer interfacial mixing. The spectral shape of the EQE of P3HT/PCBM bilayers calculated by combining the exciton generation profile in the cell with one-dimensional exciton diffusion, resembles the experimental data of the as-cast bilayer but does not reproduce its magnitude. This indicates that P3HT/PCBM bilayers made using regioregular P3HT via orthogonal solution processing lead to bi-layer-like morphologies that are partly intermixed at the interface. Thermal annealing enhances the depth of PCBM segregation and hence percolation and converts the layer into a bulk heterojunction. For thick (≥80 nm) P3HT films, the performance of the annealed P3HT/PCBM bilayers is significantly better that of corresponding solution cast bulk heterojunctions. This is consistent with the recent result that annealing of bilayers provides a morphology that has a percolating PCBM network throughout the P3HT layer, but is not intimately mixed.[11]

ASSOCIATED CONTENT

Supporting Information. Details on the optical constants and optical modeling (PDF). This material is available free of charge via the Internet at http://pubs.acs.org.

AUTHOR INFORMATION

Corresponding Author
*E-mail: r.a.j.janssen@tue.nl.

ACKNOWLEDGMENT

The work is part of the research program of the Dutch Polymer Institute (DPI project 660) and further supported by the Deutsche Forschungsgemeinschaft under Priority Programme 1355.

REFERENCES

(1) Yu, G.; Gao, J.; Hummelen, J. C.; Wudl, F.; Heeger, A. J. *Science* **1995**, *270*, 1789–1791.
(2) Thompson, B.; Fréchet, J. *Angew. Chem., Int. Ed.* **2008**, *47*, 58–77.
(3) Yang, X.; Veenstra, S. C.; Verhees, W. J. H.; Wienk, M. M.; Janssen, R. A. J.; Kroon, J. M.; Michels, M. A. J.; Loos, J. *Nano Lett.* **2005**, *5*, 579–583.
(4) Ayzner, A. L.; Tassone, C. J.; Tolbert, S. H.; Schwartz, B. J. *J. Phys. Chem. C* **2009**, *113*, 20050–20060.
(5) Wang, D. H.; Choi, D-G; Lee, K.-J.; Im, S. H.; Park, O. O.; Park, J. H. *Org. Electron.* **2010**, *11*, 1376–1380.
(6) Collins, B. A.; Gann, E.; Guignard, L.; He, X.; McNeill, C. R.; Ade, H. *J. Phys. Chem. Lett.* **2010**, *1*, 3160–3166.
(7) Treat, N. D.; Brady, M. A.; Smith, G.; Toney, M. F.; Kramer, E. J.; Hawker, C. J.; Chabinyc, M. L. *Adv. Energy Mater.* **2011**, *1*, 82–89.
(8) Chen, D.; Nakahara, A.; Wei, D.; Nordlund, D.; Russell, T. P. *Nano Lett.* **2011**, *11*, 561–571.
(9) Moon, J. S.; Takacs, C. J.; Sun, Y.; Heeger, A. J. *Nano Lett.* **2011**, *11*, 1036–1039.
(10) Lee, K. H.; Schwenn, P. E.; Smith, A. R. G.; Cavaye, H.; Shaw, P. E.; James, M.; Krueger, K. B.; Gentle, I. R.; Meredith, P.; Burn, P. L. *Adv. Mater.* **2011**, *23*, 766–770.
(11) Chen, C.; Liu, F.; Wang, C.; Nakahara, A.; Russell, T. P. *Nano Lett.* **2011**, *11*, 2071–2078.
(12) Germack, D. S.; Chan, C. K.; Kline, R. J.; Fischer, D. A.; Gundlach, D. J.; Toney, M. F.; Richter, L. J.; DeLongchamp, D. M. *Macromolecules* **2010**, *43*, 3828–3836.
(13) Cook, S.; Furube, A.; Katoh, R.; Han, L. *Chem. Phys. Lett.* **2009**, *478*, 33–36.
(14) Cook, S.; Liyuan, H.; Furube, A.; Katoh, R. *J. Phys. Chem. C* **2010**, *114*, 10962–10968.
(15) Markov, D. E.; Blom, P. W. M. *Phys. Rev. B* **2005**, *72*, 161401(R).
(16) Theander, M.; Yartsev, A.; Zigmantas, D.; Sundström, V.; Mammo, W.; Andersson, M. R.; Inganäs, O. *Phys. Rev. B* **2000**, *61*, 12957–12963.